ERROR ANALYSIS FOR MEASUREMENT OF TISSUE ELASTIC CONSTANT AND ITS PRACTICAL APPLICATION

KEN OHARA and SADAYUKI SAKUMA

Department of Radiology Nagoya University School of Medicine
(Director: Prof. Sadayuki Sakuma)

ABSTRACT

This paper examined the availability of a method for calculating the "mean elastic constant" of tissue and its practical applicability. The error analysis for the elastic constant of tissue was obtained by theoretical and experimental methods. Its error depends on measured lengths from Computerized Tomograms (CT), Ultrasonograms (US), CT-values and their deviations. This method can be accurately applied to soft tissue and organs of 4 cm or more with an error of less than 20% *in vivo* with the exception of bone, lungs, and gas filled organs. The procedure we employed for obtaining the "mean elastic constant" by combining CT with US is presented.

Keywords: Tissue Characterization, Mean Elastic Constant, Computerized Tomography, Ultrasonography.

INTRODUCTION

Ultrasound images are produced by reflected sound waves or echoes from tissue whose acoustic impedance is different from its surrounding tissues. The distance between the transducer and a point in the tissue is obtained by monitoring the time which the acoustic waves take to reach their target and return to the transducer[1~8]. Most medical ultrasound diagnostic equipment has an adjusted sound speed of about 1,540 m/s as a standard velocity for soft tissue. When the sound passes through the tissue, and is reflected at a different velocity from the standard, a distorted image will be obtained, and the length between the two points in the tissue will differ from the actual distance.

The density of tissue, ρ, the bulk modulus K, and the acoustic velocity V, are quantities that are related to each other through the following equation[9]:

$$V = \sqrt{K/\rho} \tag{1}.$$

This relationship shows that the bulk modulus can be obtained if the sound velocity and the density are known. It is expected that one of the tissue properties can be quantified if the bulk modulus is obtained.

We have developed a new equation which can calculate a tissue's "means elastic constant" instead of its bulk modulus by obtaining the measured distances from *in vivo* Computerized Tomograms (CT)[10] and Ultrasonograms (US), and CT-values (see, Companion paper). The availability of the equation in the companion paper was examined by means of an error

---

小原　健・佐久間貞行

theory, and newly developed data processing system which, along with its practical application, is presented in this study.

ERROR ANALYSIS OF THE BASIC EQUATION AND MEASUREMENT

1. Basic Equation and its Error Evaluation

The basic equation calculating the elastic constant is shown as:

$$K_t = K_w \frac{L_c^2}{L_u^2} (1 - \frac{N_c}{N_{air}}) \tag{2}.$$

where K_t is an elastic constant, and K_w is the bulk modulus of water, L_c is a measured CT image length, and L_u is a measured US image distance. N_c and N_{air} are the CT-values of tissue and air respectively when N_{air} is $-1,000$ and N_{water} is $0^{11)}$. If the standard sound velocity in water is taken at 1,530 m/s regardless of the velocity in tissue, K_t can be calculated by using L_c, L_u, and N_c.

Equation (2) is partially differentiated with respect to L_c, L_u, and N_c in evaluating the accuracy of the error in K_t. The error equation divided by K_t is written as follows:

$$\frac{\Delta K_t}{K_t} = \frac{2}{L_u} \Delta L_u + \frac{2}{L_c} \Delta L_c + \frac{\Delta N_c}{(N_{air} - N_c)} \tag{3}.$$

where, ΔL_u, ΔL_c, and ΔN_c are variations of L_u, L_c, and N_c respectively. It is considered that ΔL_u is the error of measured length from a US image, ΔL_c is one from a CT image, and ΔN_c is a Root Mean Square (RMS) or Standard Deviation (SD) of the CT-values. Equation (2) has been modified for the convenience of measurement, and is rewritten as follows:

$$K_t' = K_w \frac{L_c^2}{L_u^2} (1 - \frac{\epsilon \sum_{i=1}^{n} q_i}{L_c}) \tag{4}.$$

where ϵ is the actual pixel size of a CT-display, q_i is the amount of each CT-value divided by N_{air}, ($q_i = N_{ci}/N_{air}$), n is the number of pixels along a measured length, and i is integer. Equation (3) is similarly modified and is shown as follows:

$$\frac{\Delta K_t}{K_t} = \frac{2}{L_u} \Delta L_u + \frac{|2 - \overline{q}| \Delta L_c}{L_c (1 - \overline{q})} + \frac{\overline{\Delta q}}{(1 - \overline{q})} \tag{5}.$$

$\overline{q}$ is written to replace $\epsilon \sum_{i=1}^{n} q_i/L_c$, as $\overline{q}$ is an averaged value of q_i along a measured distance.

Fig. 1a shows the error in distance measurement by US and CT, and was obtained from the first and second terms of the right member of equation (5) as a function of the rate of distance error to measured distance $\Delta L_u/L_u$ or $\Delta L_c/L_c$. The oblique solid line shows the US distance error which was calculated from the first term, or CT distance error, where $\overline{q}$ is zero from the second term. The first term is inversely related to the US distance, and the second term is in similar relation with the exception of the dependance of the rate of the mean CT-value ($\overline{N}_c$) to $\overline{N}_{air}$. The dotted lines show the CT distance error where $\overline{q}$ is 0.4 ($\overline{N}_c = -400$), 0,2 ($\overline{N}_c = -200$), -0.2 ($\overline{N}_c = 200$), and -0.4 ($\overline{N}_c = 400$). Fig. 1b shows the CT-value error from the third term as a function of the rate of mean CT-value ($\overline{N}_c$) to N_{air}, where RMS of CT-values are 10 ($\overline{\Delta q} = 0.01$), 30 ($\overline{\Delta q} = 0.03$), 50 ($\overline{\Delta q} = 0.05$), and 100 ($\overline{\Delta q} = 0.1$) respectively. This error is inevitable

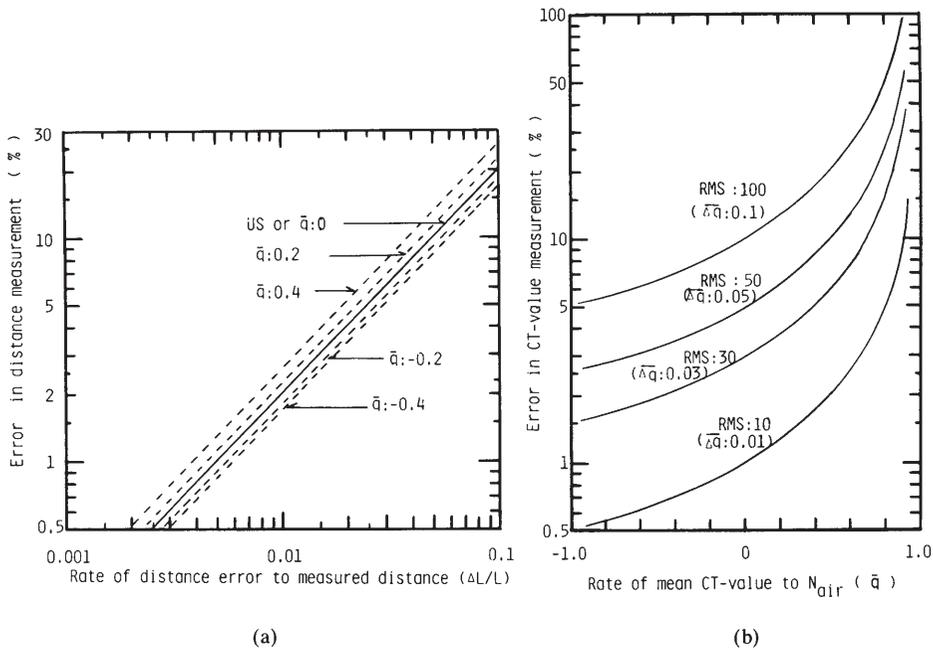(a)   (b)

Fig. 1   Percentile error calculated from equation (5).
    (a) Distance errors from US and CT as a function of the rate of the distance error to the measured
        distance. The US and CT distance error is shown by a solid line where $\bar{q}$ is zero. The dotted lines
        show the CT distance error where $\bar{q}$ is 0.4 ($\bar{N}_c = -400$), -0.2 ($\bar{N}_c = -200$), -0.2 ($\bar{N}_c = 200$), and -0.4
        ($\bar{N}_c = 400$) respectively.
    (b) Percentile CT-value error as a function of the rate of the mean CT-value ($\bar{N}_c$) to N_{air}; $\bar{q}$, where
        RMS are 100 ($\overline{\Delta q} = 0.1$), 50 ($\overline{\Delta q} = 0.05$), 30 ($\overline{\Delta q} = 0.03$), and 10 ($\overline{\Delta q} = 0.01$) respectively.

even if the distance measurements can be carried out accurately. Equation (5) expresses the
longer measured distance, the lesser CT-value, the higher tissue density, and the smaller value
of equation (5). As $\bar{q}$ approaches 1.0, the total error increases rapidly.

2.   The Determination of Actual Distance Error

The error principally depends on the pixel size of the CT display used in the distance
measurement. The pixel size is in the range of 0.5 mm to 1.5 mm, and the distance error can be
evaluated to be about twice the size of the pixel. The measured length can be written as $L_c \pm$
2ϵ[11,12].

US equipment's spatial resolution, however, is 2—4 times larger than the pixel size, and it
generally depends on acoustic frequency[13]. A simple experiment was performed to evaluate
how the frequency affected the actual error of a measured length. A US diagnostic compound
scanner (Aloka model SSD-180) was used, and the frequencies applied were 2.25, 3.5, 5.0, 7.5,
and 10.0 MHz changing the amplifier gain to the same conditions of diagnosis whenever
possible. The phantom was cylindrically shaped having a diameter of 6 cm, and the acoustic
absorber was placed in the bottom of the phantom to reduce the effects of multiple reflection.
The Full Width of Half Maximum (FWHM) of the reflected wave as an axial resolution was
measured by using an oscilloscope and changing the distance by 1.0 or 1.5 cm steps from the
transducer to a boundary layer between olive oil and the water.

Fig. 2 shows the results of the above FWHMs. Note that the higher the frequency was
raised, the better the axial resolution became. Unsatisfactory results, however, may have been
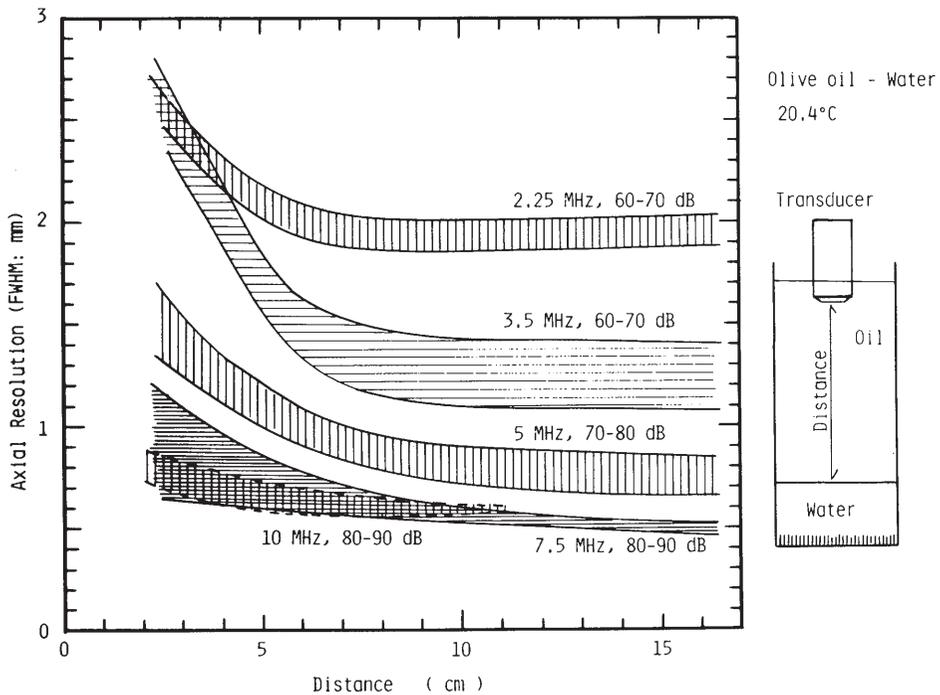
Fig. 2   Axial resolution (FWHM) for each frequency as a function of distance from the tranasducer along
the direction of its axis. Amplifier gain is set at the same conditions for diagnosis whenever possible.

the result of high frequency saturation of the US circuit. As the points became more distant
from the transducer, the axial resolution became better. Fig. 2 shows the FWHM values of
2.1, 1.7, 1.1, 0.8, and 0.7 mm in order of each frequency at a point 5 cm distant from the
transducer along the direction of its axis.

Fig. 3 shows the total percentile errors, where ΔL_u, $\Delta L_c = \pm 1.0$ mm, ± 1.5 mm, and ± 2.0 mm
in the range of mean CT-value $(\overline{N}_c)$ from $-200\,(\overline{q} = 0.2)$ to $200\,(\overline{q} = -0.2)$ with RMS $= 50\,(\overline{\Delta q} =$
0.05) as a function of measured length assuming $L_u = L_c$. The "mean elastic constant" has no
reliability for small portions of organs when the measured length is less than 3 cm, and the
total error may remain less than 20% when the length is longer than 4 cm as shown by the
middle shadowed portion in Fig. 3.

EXPERIMENT TO OBTAIN THE BULK MODULUS OF OLIVE OIL

A phantom containing liquid paraffin, olive oil, and water was used. The liquids were
selected according to their different acoustic and physical properties, *i.e.*, bulk modulus,
density, insoluability, and atomic composition. In this experiment, the bulk modulus of olive
oil was measured at a temperature of 20.4°C. Fig. 4a and 4b show the CT and US image of the
phantom respectively. The upper layer in Fig. 4a is the layer of liquid paraffin, the middle layer
is that of olive oil, and the lower one is that of water. The thickness of the olive oil layer was
measured by using CT and US images. CT-values and RMS were determined by CT software.

The thickness measured by CT was 37.0 ± 1.0 mm, which was in agreement with the real
thickness. The density calculated from the mean CT-value was 0.877 ± 0.005 g/cm^3, which
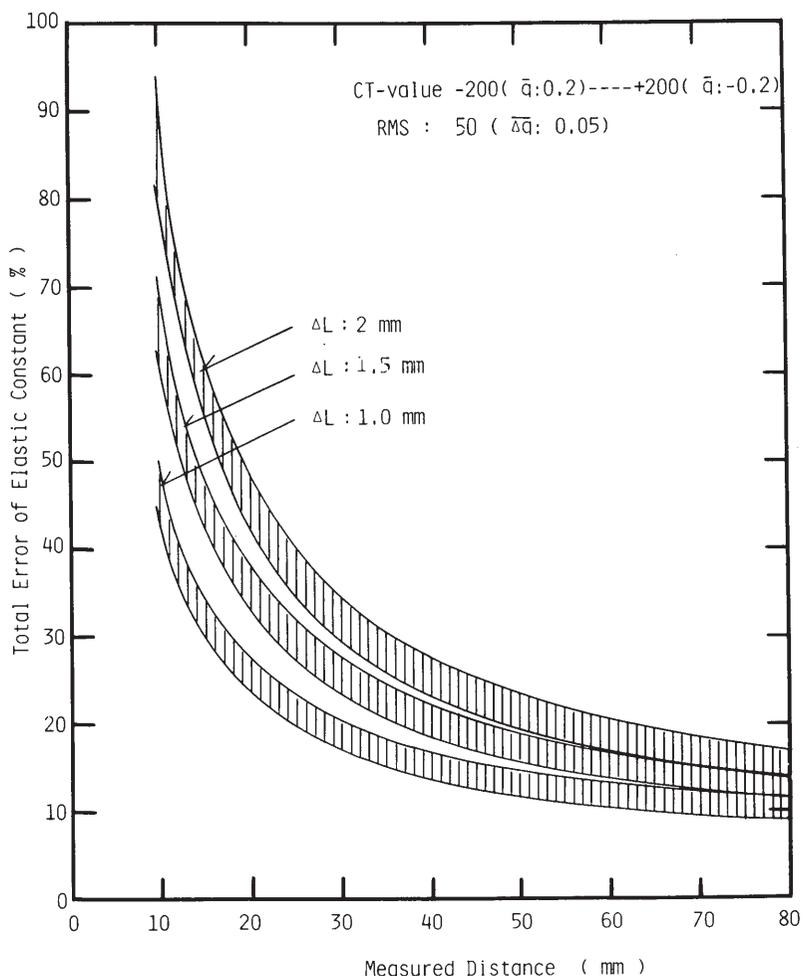was a slight underestimation in comparison with its true density of 0.906 g/cm^3 at 20.4°C due

Fig. 3 Total percentile error of the "mean elastic constant" as a function of the measured distance. CT-values −200 to +200 ($\bar{q}$: 0.2 to −0.2), RMS = 50 ($\overline{\Delta q}$ = 0.05) for each shadowed portion. Measured distances of CT, and US were assumed to be equal. Distance error ΔL: ±1.0, ±1.5, and ±2.0 mm.

to affected CT-values caused by the phantom shape. The thickness obtained from US imagery was 39.0 ± 1.0 mm setting the amplifier gain at 90 dB when the frequency was 5 MHz. Then the bulk modulus was determined as 1.8×10^9 N/m^2. Its error was estimated at about 15%. It agrees approximately with a nominal one of 1.88×10^9 N/m^2 within the experimental error[14].

DATA PROCESSING SYSTEM AND ITS PRACTICAL APPLICATION

A new processing system has been developed for determination of the "mean elastic constant" of tissue. The system is a hybrid which has combined US and CT or Independent Viewing Console (IVC) equipment. The CT image data is transferred to a CT disc and Magnetic Tape (MT) or IVC disc. The same cross sectional US imagery data is transferred to a CT disc and MT or an IVC disc in a similar process. Images from both the MT and the disc are displayed on CT and/or IV consoles. The distance measurement is performed by

<div align="center">(a)</div>
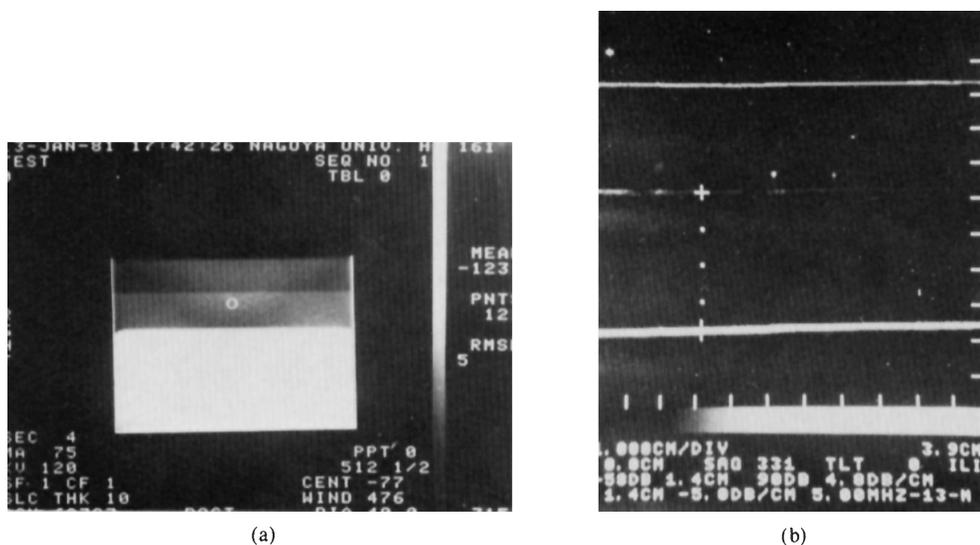

<div align="center">(b)</div>

Fig. 4   Computerized Tomogram (a) and Ultrasonogram (b) of the phantom. The phantom's upper layer of liquid paraffin; the middle layer of olive oil; and the lower layer of water. The bulk modulus of olive oil was measured.

manually designating two points on the image, thereby obtaining the mean CT-value along a measured length or in the regions of interest. Then, the "mean elastic constant" is calculated. The results are displayed on CRT and stored on MT and IVC discs.

Ease of distance measurement, and the recording of results are some of the functions included in the software system. These functions are written as follows:

1) Magnified display at a specified mangification ratio for decreasing the error of length measurement. In this mode, one of the two images (CT and US) is displayed on the monitor as shown in Fig. 5a and 5b.

2) The mean CT-value and its RMS in the regions of interest can be obtained as shown in Fig. 5c.

3) Combined display of images as shown in Fig. 5d allows easier measurement and recording.

4) A line between two designated points can be displayed, and commentary concerning image information with arrows specifying points can be written by the system's Key Board.

5) Temperature caliblation can be carried out for obtaining the "mean elastic constant" of an obtained specimen or other experimental materials.

Compound scanning is superseded by electronic linear scanning in this system as shown Fig. 5b and 5d[15]. This is because the time required to make a picture is shorter than the time required for compound scanning, and electronic linear scanning has the merits of fast processing of patients, and of easily synchronizing the respiratory phase at the period of CT exposure regardless of the compound scanning's better image quality.

Fig. 5a through 5d show a case of cirrhoris. The distance between the liver's edge and the wall of the Vene Cava was measured along the acoustic shadow of rib. The displayed number of 3.148 shown in Fig. 5d is the "mean elastic constant" of the liver multiplied by 10^9 N/m². Another display is calculated from the following formula, $100 (K_t/K_w - 1)$. The error in K_t remains less than 15%.
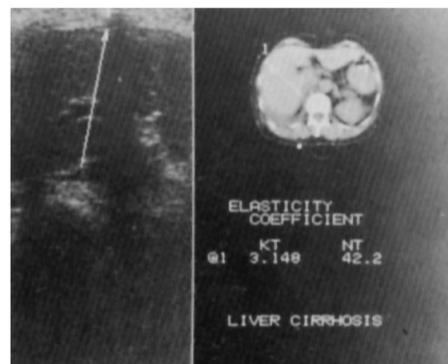
(a)
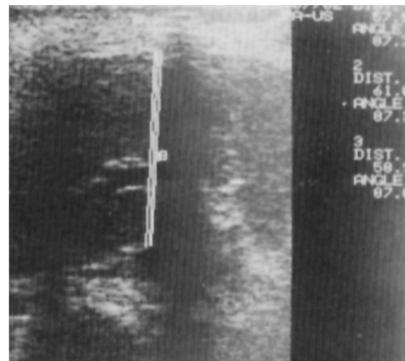
(b)

(c)

(d)

Fig. 5   A clinical case for measurement of the mean elastic constant.
(a) Magnified display of CT image.
(b) Magnified display of US image.
(c) Magnified display of CT image, mean CT-value, and its RMS are calculated in regions of interest.
(d) Combined display of reduced images. Some comments can be written through the computer's key-board.

DISCUSSION

Elasticity is a property of material which spontaneously resumes its normal shape and bulk after having been constracted, dilated, and/or distorted. Young's ratio, Poisson's ratio, bulk modulus, and rigidity are used for indicating the various elastic properties of material. These values express the force per unit area required to produce unit displacement when external force is applied to the material in different directions, and are related to each other by having had their formula determined through a common homogeneous material. Acoustic properties of simple materials can be decided easily, but acoustic properties of tissue are difficult to obtain due to the tissue's complex structure, temperature dependance, and composition. Our "mean elastic constant" of tissue may be complexly related to the above four elastic constants. However, the "mean elastic constant" can be derived on the bases of equation (1), but may also indicate the "mean bulk modulus" of tissue. As the bulk modulus of simple material relates to the change of volume when external force is applied, it can also indicate "solidity" of "hardness" of an object. It can then be considered that the "mean elastic constant" can also be used to interpret the "solidity" or "hardness" of tissue. The number 3.148 ($\times 10^9$ N/m^2) displayed in Fig. 5d is larger than the value of normal liver which is about 2.6 $\times$ 10^9 N/m^2 [16,17]. The number is a clear indication of the cirrhotic liver's tissue hardness.

The density of living tissue *in vivo* cannot be obtained easily or directly by current methods used in "tissue characterization"[18] despite the many laboratory methods that have been developed[19]. The problems involved determining the density and thickness of tissue have been solved by our method, and now the "mean elastic constant" of tissue corresponding to deep palpation can be compared.

Assurance in the calculations of the same cross CT and US sections along with, and considering, the respiratory motions of an organ is an important problem in distant measurement. One way of obtaining accurate cross sectional figures and reducing the respiratory effect is by the use of a small, thin, Pb, or low density plastic (Lucite) marker. This marker is pasted on the patient's skin as shown Fig. 5a and 5c, is visible in the CT image, and has little or no bearing on the CT-values in the regions of interest. This method is, however, imcomplete and inconvenient for obtaining many continuous "mean elastic constant" cross sections. This problem can be solved by synchronizing the respiratory phase for each cross section, and by using high speed CT scanning instead of the whole body CT scanning time of 2 seconds that is in current use. A better means of solving this problem is by taking simultaneous pictures of the same CT and US cross section through a water bag in combination with the above two methods.

Some examples of tissues that are difficult to examine due to the ultrasound being too strongly absorbed or reflected to make an image are: bone, lungs, and gas filled organs. These problems, with the exception of the brain tissue, are inevitable due to the acoustic nature of ultrasound. Another problem concerns distance measurement. The accuracy of US and CT distance measurements depends on acoustic frequency and spatial resolution, respectively. The accuracy of US distance measurements can be improved by using an A-mode scope applying high frequency and high intensity ultrasound with high attenuation ratio compensation, and by using a US circuit having wide dynamic and frequency ranges. CT spatial resolution can be improved by using magnified CT scanning whose pixel size is relatively smaller than conventional CT scanning. More accurate results can be obtained by using magnified CT scanning. If CT and US FWHMs have values of 0.1 mm the sum of errors in the distance measurements will be evaluated to be less than 8% when the measured distances are longer than 1 cm. The reliability and reproducibility of CT-values are affected

by the exposure conditions such as: potentials, current, and the size of the patient, etc. It is necessary that the CT equipment be finely adjusted[11,12,13], and that the number of pixels in the regions of interest be enough to decrease the RMS. These problems can be solved within the scope of present technology.

There are many kinds of imagery techniques in radiology. They are roentgenography, ultrasonography, radioisotope imagery, radio frequency (RF) imagery and nuclear magnetic resonance (NMR) imagery. These techniques show the respective properties of tissue and/or organs such as: X-ray attenuation due to tisisue density or its electron density, the difference in acoustic impedance, uptake of radiopharmaceuticals in tissue, dielectric loss of tissue, and the proton denisty or the ^{31}P density of tissues. The data of these images can be fed into the computer facilitating the comparison of this information with each other. Our research combines US and CT, with the "mean elastic constant" allowing new medical information to be derived. Some examples of the application of our combined techniques are calculation of the water density of tissue using CT and NMR, and determination of the dielectric constant of tissue using CT and RF imaging.

CONCLUSION

The distance required to measure soft tissue using present CT and US equipment with an error of less than 20% is 4 cm. Our method makes available *in vivo* measurement of the "mean elastic constant" of tissue with the exception of organs such as bone, lung, gas filled organs, and areas where acoustic waves are too strongly absorbed or reflected to make an image.

Data processing systems are convenient for quick data acquisition, calculation, and recording.

Some methods for obtaining a more accurate "mean elastic constant", and the possibility of coming up with new medical information by using our combined technique have been discussed.

It is our considered opinion that the "mean elastic constant" of tissue will become one of the medicine's new diagnostic tools.

ACKNOWLEDGEMENT

REFERENCES

1) French, L. A., Wild, J. J., and Neal. D.: DETECTION OF CEREBRAL TUMORS BY ULTRASONIC PULSES, Pilot Studies on Postmortem Material. *Cancer*, 3, 705—708, 1950.

2) Howry, D. H., and Bliss, W. R.: ULTRASONIC VISUALIZATION OF SOFT TISSUE STRUCTURES OF THE BODY, *J. Lab. Clin. Med.*, **40**, 579—592, 1952.

3) Wild, J. J., and Reid, J. M.: The Effects of Biological Tissues on 15-mc Pulsed Ultrasound, *J. Acous. Soc. Am.*, **25**, (2), 270—280, 1953.

4) Wild, J. J., and Reid, J. M.: Echographic Visualization of Lesions of the Living Intact Human Breast, *Cancer Res.*, **14**, 277—283, 1954.

5) Kikuchi, Y., Uchida, R., Tanaka, K., *et al.*: Early Cancer Diagnosis through Ultrasonics, *J. Acous. Soc. Am.*, **29**, (7), 824—833, 1957.

6) Wagai, T.: Ultrasound Tomography, *Geka*, **22**, (12), 1205—1217, 1960 (in Japanese).

7) de Vlieger, M., de Sterke, A., Molin, C. E., *et al.*: ULTRASOUND FOR TWO-DIMENSIONAL ECHO-ENCEPHALOGRAPHY, *Ultrasonics*, **1**, July- Sept., 148—151, 1963.

8) Grossman, C. C.: ACOUSTIC PHENOMENA IN ULTRASONIC DETECTION OF BRAIN TUMORS, *Ultrasonics*, **3**, Jan.-March, 22—24, 1965.

9) Nakagawa, T.: Rheology, Iwanami Zensho 249, 13—36, Iwanami-Shoten Tokyo, 1960 (in Japanese).

10) Hounsfield, G. N.: Computerized transverse axial scanning (Tomography) Part 1, Description of system, *Brit, J. Radiol.*, **46**, 1016—1022, 1973.

11) McCullough, E. C., Payne, J. T., Baker, H. L., *et al.*, Performance Evaluation and Quality Assurance of Computed Tomography Scanners with Illastrations from the EMI, ACTA, and Delta Scanners, *Radiology*, **120**, 173—188, 1976.

12) Endo, M., Takenaka, E., and Iinuma, T., *et al.*: Intercomparison of CT-scanner Imaging Quality (1), *Nipp. Acta. Radiol.*, **38**, (1), 33—41, 1978 (in Japanese).

13) Mano, I., Kaneko, M. and Takenaka, E.: Fundamental Studies of Computerized Tomography (5th part) Noise, Contrast Resolving Power, Linearity, MTF, and High Contrast Resolving Power (For Eight Models of Scanners), *Nipp. Acta. Radiol.*, **39**, (3), 284—289, 1979 (in Japanese).

14) Mitsuyoshi, J., Kikuchi, Y., and Yoshimoto, O.: Choonpa Binran, pp. 1241—1244, Nippon Kogyo Shinbunsha, Tokyo, 1966 (in Japanese).

15) Hagen-Ansert, S. L.: Textbook of Diagnostic Ultrasound Sonography, pp. 18—19, C. V. Mosby Company, St. Louis, 1978.

16) Goldman, D. E., and Hueter, T. E.: Tabular Data of the Velocity and Absorption of High-Frequency Sound in Mammalian Tissues, *J. Acous. Soc. Am.*, **28**, (1), 35—37, 1956.

17) Parry, R. T., and Chivers, R. C.: Data of the Velocity and Attenuation Ultrasound in Mammalian Tissue —A Survey—, pp. 343—360, *Ultrasonic Tissue Characterization* II, Edited by M. Linzer, NBS Special Publication 525, National Bureau of Standards, Washigton, 1979.

18) Chivers, R. C.: Tissue Characterization, *Ultrasound in Med. & Biol.*, **7**, 1—20, 1981.

19) Wells, P. N. T., Mountford, R. A., Halliwell, M. *et al.*: Quantitative A-scan analysis of normal and cirrhotic liver, in *Ultrasonic Tissue Characterization*, pp. 61—70, Edited by M. Linzer, NBS Special Publication 453, National Bureau of Standards, Washington, 1976.